JPET Fast Forward. Published on August 17, 2006 as DOI: 10.1124/jpet.106.110080

JPET #110080

Properties of a Time-dependent Potassium Current in Pig Atrium – Evidence for a Role of Kv1.5 in Repolarization

Joachim R. Ehrlich, Christin Hoche, Pierre Coutu,

Christiane Metz-Weidmann, Werner Dittrich, Stefan H. Hohnloser,

Stanley Nattel, Heinz Gögelein

Division of Cardiology, J.W. Goethe-University, Frankfurt, Germany (JRE, CH, SHH)

Research Center and Department of Medicine, Montreal Heart Institute and University of Montreal, Montreal, Quebec, Canada (PC, SN)

Genomic sciences, Sanofi-Aventis, Frankfurt, Germany (CMW, WD)

Department of Pharmacology and Therapeutics, McGill University, Montreal, Quebec, Canada (SN)

Sanofi-Aventis Deutschland GmbH, Frankfurt, Germany (HG)

JPET #110080

Running title: Kv1.5-based porcine outward current

Correspondence:

Joachim R. Ehrlich, MD

Division of Cardiology, J.W. Goethe-University

Theodor Stern Kai 7, 60590 Frankfurt, Germany

Tel.: +49 69 6301 83661, Fax: +49 69 6301 4037

Email: j.ehrlich@em.uni-frankfurt.de

text pages: 21

tables: 1

figures: 6

references: 40

abstract: 245 words

introduction: 446 words

discussion: 1299 words

Nonstandard abbreviations:

$I_{K,PO}$ – porcine outward potassium current, 4-AP – 4-aminopyridine, APD – action potential duration, BDS – blood depressing substance, E_{rev} – reversal potential, HPTX – heteropodatoxin, HTX – hongatoxin, IC_{50} – 50% inhibitory concentration, TEA – tetraethylammonium, TP – test potential

Section: cardiovascular

JPET Fast Forward. Published on August 17, 2006 as DOI: 10.1124/jpet.106.110080
This article has not been copyedited and formatted. The final version may differ from this version.

Abstract

Cardiac electrical activity is modulated by potassium currents. Pigs have been used for anti-arrhythmic drug-testing, but only sparse data exist regarding porcine atrial ionic electrophysiology. Here, we used electrophysiological, molecular and pharmacological tools to characterize a prominent porcine outward K^+ current (termed $I_{K,PO}$) in atrial cardiomyocytes isolated from adult pigs. $I_{K,PO}$ activated rapidly (time-to-peak at +60 mV: 2.1±0.2 ms), inactivated slowly (τ_f=45±10, τ_s=215±28 ms) and showed very slow recovery (τ_f=1.54±0.73 sec; τ_s=7.91±1.78 sec, n=9, 36° C). Activation and inactivation were voltage-dependent and current properties were consistent with predominant K^+-conductance. Neurotoxins (heteropodatoxin, hongatoxin, BDS) that block Kv4.x, Kv1.1, 1.2, 1.3 and 3.4 in a highly-selective manner, as well as H_2O_2 and TEA, did not affect the current. Drugs with Kv1.5-blocking properties (flecainide, perhexiline and the novel atrial-selective anti-arrhythmic AVE0118) inhibited $I_{K,PO}$ (IC_{50} 132±47, 17±10 and 1.25±0.62 μM, respectively). 4-Aminopyridine suppressed the current and accelerated its decay, reducing charge-carriage with an IC_{50} of 39±15 μM. Porcine-specific Kv channel-subunit sequences were cloned to permit real-time quantitative RT-PCR on RNA extracted from isolated cardiomyocytes, which showed much greater abundance of Kv1.5 mRNA compared to Kv1.4, Kv4.2 and Kv4.3. Action potential recordings showed that $I_{K,PO}$-inhibition with 0.1 mM 4-AP delayed repolarization (e.g., APD at -50 mV increased from 45±9 to 69±5 ms at 3 Hz, P<0.05). In conclusion, porcine atrium

JPET Fast Forward. Published on August 17, 2006 as DOI: 10.1124/jpet.106.110080
This article has not been copyedited and formatted. The final version may differ from this version.

displays a current that is involved in repolarization, inactivates more slowly than classical I_{to}, is associated with strong Kv1.5 expression and shows a pharmacological profile typical of Kv1.5-dependent currents.

Introduction

Atrial fibrillation (AF) is a very common arrhythmia contributing to morbidity and mortality of affected patients (Wolf *et al*., 1998). Medical treatment remains a mainstay of therapy (Nattel and Opie, 2006), although the use of anti-arrhythmic drugs is limited by potentially deleterious side effects (Hohnloser and Singh, 1995). Porcine models have been used to test Kv1.5-targeting atrial-selective drugs that are designed to circumvent this proarrhythmic risk inherent to treatment with conventional anti-arrhythmic drugs (Wirth *et al*., 2003). However, to date there has been no clear demonstration of Kv1.5-related currents in porcine atrium.

Potassium currents (in particular I_{to} and I_{Kur}) are among the targets of novel atrial-selective drugs developed for treating atrial-fibrillation (Knobloch *et al.*, 2004). Kinetic differences of activation, inactivation and recovery from inactivation discriminate between various potassium currents and are related to properties of the underlying ion-channel subunits. The properties of transient outward currents (I_{to}) have been characterized extensively in many species (Patel and Campbell, 2005). Fast-inactivating I_{to} ($I_{to,f}$) is carried by Kv4.3 subunits in dog and man, while Kv1.4 subunits contribute to $I_{to,f}$ in rabbit atria (Wang *et al*., 1999; Patel and Campbell, 2005). Rabbit I_{to} is characterized by particularly slow recovery from inactivation, which is related to the participation of Kv1.4 subunits (Wang *et al.*, 1999). In human atrium, I_{Kur} is carried by Kv1.5 subunits - a member of the delayed rectifier current family - and has been shown to inactivate

slowly over a period of seconds (Nattel *et al*., 1999; Feng *et al*., 1998). At room temperature, I_{Kur} may show a non-inactivating phenotype (Li *et al.*, 2004) although recording conditions importantly modulate inactivation kinetics of this current (Snyders *et al.*, 1993). Similarly, beta-subunits may modify inactivation properties of Kv1.5 currents (Uebele *et al.*, 1996).

Porcine atrial cellular electrophysiology has been studied to a limited extent and is poorly understood, although this species is commonly used in experimental studies (Janse *et al.*, 1998). A recent investigation demonstrated the presence of a Ca^{2+}-dependent chloride current ($I_{to,2}$) and I_{Kur} in porcine atria (Li *et al.*, 2004). In preliminary studies we noted a robust time-dependent current in porcine atrium that activates rapidly (like I_{Kur}) and inactivates more slowly than classical I_{to} and somewhat more rapidly than previously-reported I_{Kur}. This study aimed to characterize this porcine outward current (which we will abbreviate $I_{K,PO}$) with respect to electrophysiological properties, expression of potential corresponding underlying subunit transcripts, pharmacological responses and functional role. In particular, we were interested in studying the pharmacological profile of the current with respect to known selective blockers of potential underlying K^+-channel subunits, with a view to determining whether $I_{K,PO}$ can potentially account for previous reports of anti-AF actions of Kv1.5 blockers in pig hearts.

Methods

Animal and Tissue Handling

Male castrated pigs of the German landrace (n=62, 19±0.5 kg) were anaesthetized with intravenous application of pentobarbital (30 mg/kg). During deep anaesthesia, hearts were excised via left thoracotomy resulting in humane euthanasia. Hearts were immediately immersed in oxygenated Tyrode solution. All procedures followed the *Guide for the Care and Use of Laboratory Animals* of the NIH (publication No. 85-13, revised 1996) and were performed by technicians specifically trained and experienced in animal care.

For isolation of single cardiomyocytes, the proximal circumflex coronary artery was cannulated and the atrial preparation was perfused with oxygenated Tyrode solution on a Langendorff apparatus. The perfusion solution was then switched to Ca^{2+}-free Tyrode until all contraction ceased (~10 min) and collagenase (100 U/ml, Worthington, type II)-containing Ca^{2+}-free Tyrode solution was used for cell isolation as reported previously (Gogelein *et al.*, 2004). After isolation, cells were stored in a high-[K^+] storage solution at room temperature and studied within 12 hours. Only healthy-appearing cells with clear cross-striations and sharp edges were used for electrophysiological measurements.

For real-time RT-PCR measurements, aliquots of isolated atrial cardiomyocytes were used, while the remainder of the cell isolation was used for electrophysiological experiments on the same days.

Solutions and drugs

The high-[K^+]-containing cell-storage solution contained (mM) KCl 20, KH_2PO_4 10, dextrose 10, mannitol 40, L-glutamic acid 70, β-OH-butyric acid 10, taurine 20, EGTA 10 and 0.1% BSA (pH 7.3, KOH). Tyrode (extracellular) solution contained (mM) NaCl 136, KCl 5.4, $MgCl_2$ 1, $CaCl_2$ 1, NaH_2PO_4 0.33, HEPES 5 and dextrose 10 (pH 7.35 at 36°C, NaOH). $CdCl_2$ (200 µM, Sigma) and HMR 1556 (1 µM, Sanofi-Aventis (Gerlach *et al.*, 2001)) were added to suppress $I_{Ca,L}$ and I_{Ks}. I_{Na} contamination was avoided by using a 50-ms pre-pulse to -50 mV or by substitution of equimolar Tris-HCl for external NaCl. The internal solution for current recording contained (mM) K-aspartate 110, KCl 20, $MgCl_2$ 1, MgATP 5, Li-GTP 0.1, HEPES 10, Na-phosphocreatine 5 and EGTA 5 (pH 7.3, KOH). For action potential (AP) recording, EGTA was omitted. Fresh solutions were prepared daily. Drugs were from Sigma unless otherwise indicated and toxins from Alomone. Stock solutions were initially prepared and used throughout the study; for individual experiments cells were incubated until steady state current inhibition or washout was reached. Toxin-containing solutions were prepared freshly on each day of experimentation.

Data Acquisition and Analysis

Currents were recorded in voltage-clamp mode with whole-cell patch-clamp at 36±0.5°C (Gogelein *et al.*, 2004). Data sampling was performed at 1 kHz and filtering was at 250 Hz. Borosilicate glass electrodes had tip-resistances between 1.5 and 3.0 MΩ when filled with internal solution. Mean±SEM compensated

series-resistance was 5.6±0.1 MΩ. Cell capacitance averaged 47.6±1.9 pF (n=141). To control for cell-size variability, currents were expressed as densities (pA/pF). Junction potentials between bath and pipette solution averaged 3.6±0.5mV. APs were recorded in current-clamp mode and elicited with 2-ms twice threshold depolarizations.

Non-linear algorithms were used for curve-fitting. T-tests were used for 2-group statistical comparisons. $P<0.05$ indicated statistical significance. Data are expressed as mean±SEM.

Cloning of porcine Kv channel-subunits

To define primers for real-time RT-PCR, partial DNA sequences for pig Kv4.3 (*KCND3*), Kv4.2 (*KCND2*), Kv1.4 (*KCNA4*), and KChIP2 (*KCNIP2*) were identified. The complete sequence for porcine Kv1.5 (*KCNA5*) has been reported (NM001006593) (Gogelein *et al.*, 2004). PCR was first performed on pig brain (for *KCND3, KCND2, KCNA4)* or heart (for *KCNIP2*) cDNA with degenerate primers based on sequences from other species. Pig-specific sequences were then used to design primers (Table 1) to amplify 660 bp (*KCND3*), 532 bp (*KCND2*), 630 bp (*KCNA4*) and 591 bp (*KCNIP2*) cDNA fragments. The fragments were cloned into pCRIIblunt or pCR2.1Topo vectors and sequenced (GenBank accession numbers DQ285632 (*KCND3*), DQ285631 (*KCND2*), DQ285633 (*KCNA4*) and DQ285634 (*KCNIP2*)).

Quantitative real-time RT-PCR

Isolated cardiomyocytes were homogenized (Mixermill 300, Qiagen) and total RNA was extracted (Qiagen). DNase digestion was performed with 10 µg RNA, 5 µl 10x DNase Buffer (Ambion), 1 µl RNase Inhibitor (Applera) and 1 µl DNaseI (Ambion, 2 U μl^{-1}) in 50 µl. cDNA synthesis was performed from 2 µg RNA (Reverse Transcriptase Kit, Applera). Samples were incubated at 25°C for 10 min and 42°C for 60 min. The reaction was stopped by heating to 95°C for 5 min.

The RT product was then used as a template for subsequent PCR with gene-specific primers (Table 1). Real-time PCR was performed using an ABI Prism 7900 (Applera) and the following conditions: 2 min 50°C, 10 min 95°C, 40 cycles 95°C for 15 sec and 1 min at 60°C. Multiplex PCR used 0.125 µl target probe (50 µM), 0.45 µl target forward primer (50 µM), 0.45 µl target reverse primer (50 µM), 12.5 µl TaqMan 2x PCR master mix (Applera), 1.25 µl 20x target primers and probes (Pre-Developed TaqMan Assay Reagents, 18S rRNA control, Applera), 10 µl cDNA sample (1:20 diluted with water) or used undiluted. RNA abundance was expressed as $\Delta\Delta$Ct, Kv subunit-expression normalized to that of the internal control (18S) (Bustin, 2005).

Results

Voltage- and time-dependence

One-second depolarizing pulses from a holding potential of -80 mV to potentials between -60 and +60 mV (0.1 Hz, Fig. 1A) elicited rapidly-activating outward currents showing time-dependent inactivation. Based on this observation and further evidence detailed below we termed this current $I_{K,PO}$ for porcine outward potassium current. $I_{K,PO}$-amplitude was quantified as the difference between peak and end-pulse steady-state current unless stated otherwise. Threshold to current activation was positive to -20 mV and myocytes had a mean±SEM $I_{K,PO}$-density of 11.6±1.6 pA/pF upon depolarization to +60 mV (n=20, Fig. 1B).

Inactivation voltage-dependence was examined with 1,000-ms pre-pulses followed by 750-ms test-pulses to +60 mV (n=10 cells, Fig. 1C). Current amplitudes were normalized to current at -100 mV and plotted against the voltage of the conditioning pulse. Activation voltage-dependence was determined from the $I_{K,PO}$-voltage relationship, corrected for driving force according to the equation $a_V = I_V / (I_{max}(V-E_{rev}))$, where a_V and I_V are the activation variable and $I_{K,PO}$-amplitude at voltage V, I_{max} is $I_{K,PO}$ amplitude at +60 mV and E_{rev} was -69.2±2.3 mV (obtained from deactivating tail currents recorded at potentials between -100 mV and -60 mV after brief, ~2-5 ms, depolarizations to +60 mV). E_{rev} was corrected for liquid junction potentials. Voltages for half-maximal activation and inactivation (Boltzman fits), and corresponding slope factors were 16.8±3.8 mV (slope: 15.4±1.7) and -28.2±2.9 mV (slope: -6.1±1.5).

JPET Fast Forward. Published on August 17, 2006 as DOI: 10.1124/jpet.106.110080
This article has not been copyedited and formatted. The final version may differ from this version.

Current activation-speed assessed as time to peak was voltage-dependent and became faster at more positive potentials (e.g. 13.5±1.8 ms at 0 mV, 2.1±0.24 ms at +60 mV, Fig. 1E). Inactivation kinetics were best fitted by bi-exponential functions and resulting time-constants (τ) were slow (e.g. at +60 mV τ_f averaged 45±10 and τ_s was 215±28 ms, n=10, Fig. 1E).

Recovery from inactivation was assessed with a paired-pulse protocol with depolarizations (P1, P2) to +60 mV at increasing P1-P2 intervals (Fig. 1F) and a holding potential of -80 mV. Current during P2 was normalized to current during P1 and showed bi-exponential recovery with time-constants of 1.54±0.73 s (τ_f) and 7.91±1.78 s (τ_s, n=9, Fig. 1G).

To study frequency-dependence, cells were repetitively depolarized from -80 to +60 mV (410-ms pulses) in TrisCl-containing, Na^+-free external solution. Currents during the 10th pulse were normalized to current during the 1st pulse, showing a frequency-dependent decline (n=15, Fig. 1H). Similar experiments were performed in the presence of extracellular NaCl with 50-ms pre-pulses to -50 mV to inactivate I_{Na}. These recordings showed slightly greater frequency-dependence, but were qualitatively comparable to those obtained with TrisCl (n=7, Fig. 1H). In TrisCl, $I_{K,PO}$ elicited with the 10th pulse were 46±3% (0.5 Hz) of P1, declining to 13±3% (2 Hz), compared with 38±3% (0.5 Hz) and 7±1% (2 Hz) in NaCl-containing solution (*P*=0.07 and 0.05, respectively). The effect of equimolar Na^+ replacement by Tris and pre-pulse protocols to inactivate I_{Na} in Na^+ containing solution on peak to steady-state current was subtle. In 9 cells, $I_{K,PO}$ at +60 mV without pre-pulses averaged 8.3±1.4 and 9.5±1.4 pA/pF (*P*=NS)

JPET Fast Forward. Published on August 17, 2006 as DOI: 10.1124/jpet.106.110080
This article has not been copyedited and formatted. The final version may differ from this version.

in the presence and absence of extracellular Na^+, respectively. In Na^+ containing Tyrode currents recorded at +60 mV with 50-ms pre-pulses to -50 mV, averaged 8.4±1.5 compared with 9.3±1.4 pA/pF without pre-pulses (*P*=NS).

Effects of Cl^- and K^+ substitution on $I_{K,PO}$

To asses the potential charge carrier of $I_{K,PO}$, we investigated the effects of Cl^- and K^+ substitution on the current under study. The reversal potential of the current averaged -69.2±2.3 mV (n=3 cells). After correction for liquid-junction potentials this value was ~72 mV, compatible with a predominantly K^+-carried conductance.

$I_{K,PO}$ was also recorded in individual cells before and after replacement of external chloride by equimolar cyclamate to assess potential contributions of a previously described Ca^{2+}-dependent Cl^- current (Li, Sun, To, Tse, and Lau, 2004). This intervention did not alter $I_{K,PO}$ (Fig. 2A, B). Mean±SEM $I_{K,PO}$-density was similar over a range of voltages, averaging 7.1±1.8 pA/pF at +60 mV in NaCl and 7.0±1.9 pA/pF with Na-cyclamate (n=5, *P*=NS, Fig. 2C). The effects of intracellular K^+ replacement by Cs^+ were then determined. Currents were recorded from 10 cells with regular internal solution and from 9 other cells isolated from the same pigs on the same days with equimolar substitution of CsCl for internal KCl. Intracellular K^+-removal abolished $I_{K,PO}$: currents at +60 mV averaged 12.1±0.9 pA/pF (KCl) vs. 0.2±0.05 pA/pF (CsCl, *P*<0.001, Fig. 2F). Taken together, these results strongly suggest that $I_{K,PO}$ is primarily a K^+-current.

JPET Fast Forward. Published on August 17, 2006 as DOI: 10.1124/jpet.106.110080
This article has not been copyedited and formatted. The final version may differ from this version.

Pharmacological characterization

After having characterized the current as a K^+-dependent current with slow inactivation and recovery from inactivation, we set out to obtain the pharmacological profile of $I_{K,PO}$.

The K^+-channel blocker 4-aminopyridine (4-AP) was applied at concentrations between 0.1 µM and 100 mM. The left panel of Fig. 3A illustrates 4-AP effects on $I_{K,PO}$. Reversible suppression was seen, with a half-inhibitory concentration (IC_{50}) on peak to steady-state current of 0.81±0.16 mM (n=7, closed circles, right panel Fig. 3A). Washout returned current-amplitude to 81±5% of control. 4-AP at lower concentrations significantly accelerated current inactivation: inactivation-τ_s and -τ_f averaged was 135±70 and 35±14 ms respectively after application of 100 µM 4-AP, compared to 315±51 and 115±7 ms respectively under control conditions (P<0.05 for each), a behaviour suggestive of open-channel block (Fedida, 1997). In order to consider the reduction of charge carried by $I_{K,PO}$, we determined the 4-AP IC_{50} based on the area under the current-time curve (Dukes *et al.*, 1990; Gogelein *et al.*, 2004). Integration of the area between the remaining current at maximal 4-AP concentration and the transient outward currents for determination of FB yielded an IC_{50} of 39±15 µM (Fig. 3A, closed circles, P<0.01).

Use-dependent 4-AP-unblocking is characteristic of Kv4.2 and Kv4.3 currents (Campbell *et al*., 1993; Tseng *et al*., 1996). Currents were recorded with 400-ms pulses to +60 mV. After current stabilization, 4-AP (2 mM) was added to the bath and cells were repetitively depolarized for 10 pulses (1 Hz, n=4). There

was no significant difference between currents elicited with the first compared to the last pulse (19±7% vs. 12±8% of 1st-pulse current, *P*=NS) incompatible with use-dependent 4-AP-unblocking.

We next determined the effect of flecainide (a moderately potent blocker of Kv1 channels) on $I_{K,PO}$. Flecainide was applied at 100 nM to 1 mM (left panel of Fig. 3B) and suppressed $I_{K,PO}$ with an IC_{50} of 132±47 µM (n=10, Fig. 3B, right panel). The effect was reversible upon washout (83±12% of control). The inactivation of Kv1.4 is substantially slowed by oxidative stress as imposed by hydrogen peroxide (H_2O_2) (Dixon *et al.*, 1996). We applied H_2O_2 at an external concentration of 0.01% (Fig. 3C) and found no effect of H_2O_2 on $I_{K,PO}$ inactivation (e.g. at +60 mV τ_s=292±19 ms before vs. 299±15 ms after H_2O_2, *P*=NS). Similarly, current amplitude remained unaffected and averaged 8.4±4.5 pA/pF (at +60 mV) before versus 8.2±4.5 pA/pF after H_2O_2 arguing against a significant role for Kv1.4. Tetraethylammonium (TEA; 10 mM) did not significantly affect peak to steady-state $I_{K,PO}$, e.g. under control conditions current density at +60 mV averaged 13.6±1.6 compared to 15.0±1.7 pA/pF with TEA and 14.9±2.1 pA/pF after 15 minutes washout (Fig. 3D, n=9, *P*=NS).

Effects of specific neurotoxins

The slow inactivation of $I_{K,PO}$ made an important contribution of Kv4 subunits unlikely. To assess further any possible Kv4 contribution, heteropodatoxin (HpTX, a potent blocker of native $I_{to,1}$ and heterologously expressed Kv4 channels (Sanguinetti *et al.*, 1997) was applied at 100 and 500 nM. HpTX had no

effect on $I_{K,PO}$ (e.g. at +60 mV, mean±SEM control current density was 14.2±5.3, versus 16.2±6.7 (100 nM) and 15.9±6.6 pA/pF (500 nM, n=7, *P*=NS). Hongatoxin (HTX) blocks heterologously expressed K_V1.1, 1.2 and 1.3 channels with IC_{50}s of 31, 170 and 86 pM, respectively (Koschak *et al.*, 1998). No change in $I_{K,PO}$ was seen with 0.1 nM (e.g. at +60 mV mean±SEM $I_{K,PO}$ was 32.9±5.6 before vs. 32.5±5.8 pA/pF after HTX, respectively, n=5, *P*=NS). Blood depressing substance (BDS) is an *Anemonia sulcata*-toxin which blocks Kv3.4 transient outward currents (Diochot *et al.*, 1998). $I_{K,PO}$ density at +60 mV in 6 cells averaged 26.4±4.8 before vs. 26.7±5.0 pA/pF after application of 100 nM BDS (*P*=NS).

After the pharmacological exclusion of a significant contribution of Kv4, Kv1.1, 1.2, 1.3 and 3.4 subunits, we assessed the response to Kv1.5 blockers. We first studied the effect of perhexiline (an antianginal drug that inhibits heterologously-expressed Kv1.5 with an IC_{50} of 1.5 µM) (Rampe *et al.*, 1995). Fig. 4A depicts representative currents recorded under control conditions and in the presence of perhexiline. $I_{K,PO}$ was clearly suppressed (IC_{50}=17±10 µM, n=9, Fig. 4B). The atrial-selective compound AVE0118 (2'-{2-(4-Methoxy-phenyl)-acetylamino-methyl}-biphenyl-2-carboxylic acid (2-pyridin-3-yl-ethyl)-amide) suppresses Kv1.5 current in heterologous systems with an IC_{50} of 1.1±0.2 µM.(Gogelein *et al.*, 2004). AVE0118 inhibited $I_{K,PO}$ with an IC_{50} of 1.25±0.62 µM (Fig. 4C, D). Consistent with open-channel block, $\tau_{f.}$ accelerated from 76±18 ms (control) to 17±2 ms with 1 µM AVE0118 (n=8, *P*<0.05); whereas τ_s remained

JPET Fast Forward. Published on August 17, 2006 as DOI: 10.1124/jpet.106.110080
This article has not been copyedited and formatted. The final version may differ from this version.

unaltered (τ_s=332±26 vs. 327±53 ms for control and AVE0118, respectively, *P*=NS).

Effect of $I_{K,PO}$ inhibition on atrial action potentials

To investigate the potential physiological role of $I_{K,PO}$ in porcine atrial repolarization, we recorded effects on APs (Fig. 5A). The addition of 0.1 mM 4-aminopyridine prolonged terminal AP repolarization (Fig. 5B).

Quantitative real-time RT-PCR

Results of quantitative real-time RT-PCR on RNA extracted from isolated cardiomyocytes of animals that were also used for patch-clamp experiments demonstrated predominant expression of Kv1.5 subunit mRNA (Fig. 6A, B). Kv1.5 mRNA expression was ~15-fold that of Kv4.3 and KChIP2 (which were similar), and ~153-fold that of Kv1.4 (n=6, *P*<0.001 for each). Kv4.2 mRNA was barely detectable.

JPET Fast Forward. Published on August 17, 2006 as DOI: 10.1124/jpet.106.110080
This article has not been copyedited and formatted. The final version may differ from this version.

Discussion

Major findings

This study provides evidence for the presence of a time-dependent K^+-conductance in pig atrium with physiological properties and pharmacological responses compatible with the participation of Kv1.5 α-subunits, and a role in porcine atrial repolarization. These findings identify $I_{K,PO}$ as the likely target of Kv1.5-blockers in previous *in vivo* studies of novel antiarrhythmic compounds and suggest that pigs may represent a model for the study of atrial-selective antiarrhythmic drugs that act by inhibiting Kv1.5-based currents.

Previous studies on porcine electrophysiology

Pigs have been used for a variety of experimental studies of cardiac arrhythmias (Janse *et al.*, 1998; Wirth *et al.*, 2003), but information about the cardiac cellular electrophysiology of the pig is limited. Porcine sinoatrial cells exhibit I_{Ks} (Ono *et al.*, 2000) and ventricular myocytes exhibit an $I_{Cl,Ca}$ that contributes to repolarization (Li *et al.*, 2003). Another study by the latter investigators documented the presence of $I_{Cl,Ca}$, I_{Kur}, I_{Kr} and I_{Ks} in pig atrial myocytes (Li *et al.*, 2004). The I_{Kur} (which the authors called $I_{Kur.p}$) reported in the latter study was relatively small and apparent primarily at slow frequencies (0.05 Hz) at room temperature. $I_{Kur.p}$ showed weak inward rectification, use-dependency, 4-AP sensitivity (IC_{50}=72±4 μM) and TEA resistance. This work differs from ours in the use of low EGTA concentration in the pipette and recording at room temperature.

Our study adds to previous results in showing the presence of a substantial time-dependent outward K^+-current that is sensitive to blockers of Kv1.5, but not other possible underlying subunits, and that contributes to porcine atrial repolarization. Several lines of additional evidence presented here (including biophysical properties, as well as mRNA expression) are consistent with a potential role for underlying Kv1.5 K^+-channel subunits.

Relation of biophysical properties to other transient outward currents

The major candidate K^+-channel subunits generating rapidly activating and inactivating (so called "fast") I_{to} phenotypes are Kv4.2 and Kv4.3 (Nerbonne, 2000; Oudit *et al.*, 2001). Thus, the predominant subunit underlying native I_{to} in human ventricular cells is Kv4.3, which generates a current that inactivates rapidly as a single exponential process ($\tau_{inact.}$=7.9±0.3 ms, 35°C) (Nabauer *et al.*, 1996). Canine $I_{to,f}$ is similarly carried by Kv4.3 subunits (Dixon *et al.*, 1996). Rat ventricular I_{to} (predominantly Kv4.2) also inactivates rapidly ($\tau_{inact.}$=48±7 ms, 22°C) (Himmel *et al.*, 1999). In contrast, a functionally distinct I_{to} phenotype ($I_{to,slow}$) has been identified in many mammalian species which inactivates with a double exponential process (τ_{slow} in the order of hundreds of milliseconds) and is carried by Kv1.4 subunits (Patel and Campbell, 2005). This I_{to} phenotype is distinguished from Kv4-based currents by its slow recovery from inactivation, with time-constants of the order of seconds (Xu *et al.*, 1999; Wickenden *et al.*, 1999). For instance, ferret $I_{to,slow}$ recovers with τ=3.0±0.45 sec (at 22°C) and mouse

$I_{to,slow}$ recovers with similar time-constants (Brahmajothi *et al.*, 1999; Xu *et al.*, 1999).

Relation of biophysical properties to I_{Kur} and $I_{K,slow}$

Mouse ventricular myocytes express a current termed $I_{K,slow}$ with kinetic properties consistent with Kv1.5 *α*-subunits (Zhou *et al.*, 1998). In other species, Kv1.5 underlies the atrially-expressed ultrarapid delayed rectifier current (I_{Kur}) which is often described as non-inactivating. Although Kv1.5-current has generally been described as a delayed-rectifier, it can show substantial time-dependent inactivation, with complete inactivation for depolarizations of sufficient duration (Feng *et al.*, 1998; Lin *et al.*, 2001; Snyders *et al.*, 1993). The inactivation kinetics that we found for $I_{K,PO}$ were faster than those published for hKv1.5 in heterologous systems (e.g. τ_f=250 ms, τ_s=1500 ms; (Lin *et al.*, 2001), although the latter studies were performed at room temperature which in itself substantially slows inactivation (Snyders *et al.*, 1993). It is also possible that $I_{K,PO}$ involves a contribution of *β*-subunits, which are known to interact with Kv1.5 and accelerate its inactivation (Uebele *et al.*, 1998). A full study of the molecular biology of $I_{K,PO}$ would be very interesting but is beyond the scope of the present paper.

Pharmacological profile of $I_{K,PO}$

Kv1.5-based currents are sensitive to 4-AP. For instance, mouse ventricular $I_{K,slow}$ is inhibited by 4-AP with an IC_{50} of 32±5 µM (Zhou *et al.*, 1998). Significant

inter-species differences in 4-AP sensitivity of I_{to}s attributed to Kv1.5 exist, with IC_{50} ranging up to 600 µM in rat atrium (Zhou *et al.*, 1998). However, despite differences in affinity, all Kv1.5-carried currents are 4-AP sensitive, as was $I_{K,PO}$ in this study. Relevant $I_{K,PO}$ charge carriage inhibition (based on assessment of area under the current-time curve accounting for open channel block) occurred with an IC_{50} of 39±15 µM. IC_{50} for heterologously expressed hKv1.5 peak currents ranges between 50 and 290 µM (Bouchard and Fedida, 1995; Grissmer *et al.*, 1994), consistent with the results for $I_{K,PO}$ in the present study. While 4-AP is nonspecific in that it blocks both $I_{to,f}$ and $I_{to,s}$, the underlying mechanisms are distinct. Block of $I_{to,s}$ occurs predominantly in the open state (Campbell *et al.*, 1993). In contrast, 4-AP block of $I_{to,f}$ occurs through closed-state binding and displays use-dependent unblocking and reverse use-dependence (Patel and Campbell, 2005). No use-dependent unblocking was observed in the present study and block was consistent with open-state dependence. Both Kv1.4- and Kv1.5-currents show predominant open-state 4-AP block, but Kv1.4 is insensitive to flecanide (Akar *et al.*, 2004) and sensitive to H_2O_2, inconsistent with the response of $I_{K,PO}$. A contribution of other Kv1 subunits to $I_{K,PO}$ was excluded by the absence of any effect of hongatoxin-application. On the other hand, $I_{K,PO}$ was sensitive to perhexilene, AVE0118, flecainide and 4-AP at concentrations fully compatible with Kv1.5 inhibition (Rampe *et al.*, 1995; Gogelein *et al.*, 2004; Zhou *et al.*, 1998). A relevant contribution of Kv3.1 subunits that have been shown to underlie I_{Kur} in dogs is excluded as this current is exquisitely sensitive to TEA (IC_{50} 0.3 mM).

Potential importance of our findings

Our findings provide detailed information about the pharmacological and biophysical characteristics of a porcine outward potassium current that is a candidate to mediate the reported effects of Kv1.5-inhibiting atrial antiarrhythmic drugs (Wirth *et al.*, 2003).

Class III antiarrhythmic agents that delay atrial repolarization are effective in treating AF. However, previously-developed class III antiarrhythmic agents have prolonged atrial repolarization by blocking I_{Kr}. The untoward side-effects of I_{Kr}-inhibiting drugs include potentially lethal ventricular pro-arrhythmia (Hohnloser and Singh, 1995). The differential expression pattern of cardiac ion-channel subunits (like Kv1.5) in atria versus ventricles provides a potential basis for treatment options for atrial arrhythmias that have reduced proarrhythmic risks (Nattel *et al.*, 1999). The development of Kv1.5-based drugs as atrial antiarrhythmic agents has been limited by a lack of animal models with Kv1.5-regulated atrial repolarization. Porcine models have been used for *in vivo* testing of Kv1.5-blocking drugs, and have demonstrated potent efficacy against atrial arrhythmias without significant ventricular actions (Wirth *et al.*, 2003). $I_{K,PO}$ – as characterized in this study - contributes to atrial repolarization and has properties suggesting that it is carried by Kv1.5 α-subunits. This result provides for the first time a biophysical basis supporting the use of pigs as a model to test novel Kv1.5-inhibiting atrial-selective anti-AF agents.

Limitations of this study

Variability in cell isolation can affect the results obtained. To minimize errors introduced by this process, we studied APs and mRNA levels from cells in pigs that were used for current recordings on the same day. Furthermore, native cells express a variety of ionic currents and their electrophysiological isolation requires selective protocols and pharmacological agents with imperfect specificity. 1-sec pulses were chosen to allow for almost complete inactivation of the current. In some instances incomplete inactivation might have caused biophysical inaccuracy but longer pulses were poorly tolerated and the results had minimal effect on the analyses. Another limitation of this study is the lack of protein-expression data. We tried to obtain Western blots from porcine atrial protein preparations, but were unable to obtain specific bands with commercially available antibodies, none of which have been raised against porcine-specific epitopes.

References

Akar FG, Wu RC, Deschenes I, Armoundas AA, Piacentino V, III, Houser SR, and Tomaselli GF (2004) Phenotypic differences in transient outward K^+ current of human and canine ventricular myocytes: insights into molecular composition of ventricular Ito. *Am J Physiol Heart Circ Physiol* **286**:H602-H609.

Bouchard R and Fedida D (1995) Closed- and open-state binding of 4-aminopyridine to the cloned human potassium channel Kv1.5. *J Pharmacol.Exp.Ther.* **275**:864-876.

Brahmajothi MV, Campbell DL, Rasmusson RL, Morales MJ, Trimmer JS, Nerbonne JM, and Strauss HC (1999) Distinct transient outward potassium current (I_{to}) phenotypes and distribution of fast-inactivating potassium channel alpha subunits in ferret left ventricular myocytes. *J Gen.Physiol* **113**:581-600.

Bustin SA (2005) Real-time, fluorescence-based quantitative PCR: a snapshot of current procedures and preferences. *Expert.Rev.Mol.Diagn.* **5**:493-498.

Campbell DL, Qu Y, Rasmusson RL, and Strauss HC (1993) The calcium-independent transient outward potassium current in isolated ferret right ventricular myocytes. II. Closed state reverse use-dependent block by 4-aminopyridine. *J Gen.Physiol* **101**:603-626.

Diochot S, Schweitz H, Beress L, and Lazdunski M (1998) Sea anemone peptides with a specific blocking activity against the fast inactivating potassium channel Kv3.4. *J Biol.Chem.* **273**:6744-6749.

Dixon JE, Shi W, Wang HS, McDonald C, Yu H, Wymore RS, Cohen IS, and McKinnon D (1996) Role of the Kv4.3 K+ channel in ventricular muscle. A molecular correlate for the transient outward current. *Circ Res* **79**:659-668.

Dukes ID, Cleemann L, and Morad M (1990) Tedisamil blocks the transient and delayed rectifier K^+ currents in mammalian cardiac and glial cells. *J Pharmacol.Exp.Ther.* **254**:560-569.

Fedida D (1997) Gating charge and ionic currents associated with quinidine block of human Kv1.5 delayed rectifier channels. *J Physiol* **499**:661-675.

Feng J, Xu D, Wang Z, and Nattel S (1998) Ultrarapid delayed rectifier current inactivation in human atrial myocytes: properties and consequences. *Am J Physiol* **275**:H1717-H1725.

Gerlach U, Brendel J, Lang HJ, Paulus EF, Weidmann K, Bruggemann A, Busch AE, Suessbrich H, Bleich M, and Greger R (2001) Synthesis and activity of novel and selective I(Ks)-channel blockers. *J Med.Chem.* **44**:3831-3837.

Gogelein H, Brendel J, Steinmeyer K, Strubing C, Picard N, Rampe D, Kopp K, Busch AE, and Bleich M (2004) Effects of the atrial antiarrhythmic drug AVE0118 on cardiac ion channels. *Naunyn Schmiedebergs Arch.Pharmacol.* **370**:183-192.

Grissmer S, Nguyen AN, Aiyar J, Hanson DC, Mather RJ, Gutman GA, Karmilowicz MJ, Auperin DD, and Chandy KG (1994) Pharmacological characterization of five cloned voltage-gated K+ channels, types Kv1.1, 1.2, 1.3, 1.5, and 3.1, stably expressed in mammalian cell lines. *Mol.Pharmacol.* **45**:1227-1234.

Himmel HM, Wettwer E, Li Q, and Ravens U (1999) Four different components contribute to outward current in rat ventricular myocytes. *Am J Physiol* **277**:H107-H118.

Hohnloser SH and Singh BN (1995) Proarrhythmia with class III antiarrhythmic drugs: definition, electrophysiologic mechanisms, incidence, predisposing factors, and clinical implications. *J Cardiovasc Electrophysiol* **6**:920-936.

Janse MJ, Opthof T, and Kleber AG (1998) Animal models of cardiac arrhythmias. *Cardiovasc Res* **39**:165-177.

Knobloch K, Brendel J, Rosenstein B, Bleich M, Busch AE, and Wirth KJ (2004) Atrial-selective antiarrhythmic actions of novel I_{kur} vs. I_{kr}, I_{ks}, and I_{KAch} class Ic drugs and beta blockers in pigs. *Med.Sci.Monit.* **10**:BR221-BR228.

Koschak A, Bugianesi RM, Mitterdorfer J, Kaczorowski GJ, Garcia ML, and Knaus HG (1998) Subunit composition of brain voltage-gated potassium channels determined by hongotoxin-1, a novel peptide derived from Centruroides limbatus venom. *J Biol.Chem.* **273**:2639-2644.

Li GR, Du XL, Siow YL, O K, Tse HF, and Lau CP (2003) Calcium-activated transient outward chloride current and phase 1 repolarization of swine ventricular action potential. *Cardiovasc Res* **58**:89-98.

Li GR, Sun H, To J, Tse HF, and Lau CP (2004) Demonstration of calcium-activated transient outward chloride current and delayed rectifier potassium currents in Swine atrial myocytes. *J Mol.Cell Cardiol.* **36**:495-504.

Lin S, Wang Z, and Fedida D (2001) Influence of permeating ions on Kv1.5 channel block by nifedipine. *Am J Physiol Heart Circ Physiol* **280**:H1160-H1172.

Nabauer M, Beuckelmann DJ, Uberfuhr P, and Steinbeck G (1996) Regional differences in current density and rate-dependent properties of the transient outward current in subepicardial and subendocardial myocytes of human left ventricle. *Circulation* **93**:168-177.

Nattel S and Opie LH (2006) Controversies in atrial fibrillation. *Lancet* **367**:262-272.

Nattel S, Yue L, and Wang Z (1999) Cardiac ultrarapid delayed rectifiers: a novel potassium current family o f functional similarity and molecular diversity. *Cell Physiol Biochem.* **9**:217-226.

Nerbonne JM (2000) Molecular basis of functional voltage-gated K^+ channel diversity in the mammalian myocardium. *J Physiol* **525**:285-298.

Ono K, Shibata S, and Iijima T (2000) Properties of the delayed rectifier potassium current in porcine sino-atrial node cells. *J Physiol (Lond)* **524**:51-62.

Oudit GY, Kassiri Z, Sah R, Ramirez RJ, Zobel C, and Backx PH (2001) The molecular physiology of the cardiac transient outward potassium current (I(to)) in normal and diseased myocardium. *J Mol.Cell Cardiol.* **33**:851-872.

Patel SP and Campbell DL (2005) Transient outward potassium current, 'Ito', phenotypes in the mammalian left ventricle: underlying molecular, cellular and biophysical mechanisms. *J Physiol* **569**:7-39.

Rampe D, Wang Z, Fermini B, Wible B, Dage RC, and Nattel S (1995) Voltage- and time-dependent block by perhexiline of K^+ currents in human atrium and in cells expressing a Kv1.5-type cloned channel. *J Pharmacol.Exp.Ther.* **274**:444-449.

Sanguinetti MC, Johnson JH, Hammerland LG, Kelbaugh PR, Volkmann RA, Saccomano NA, and Mueller AL (1997) Heteropodatoxins: peptides isolated from spider venom that block Kv4.2 potassium channels. *Mol.Pharmacol.* **51**:491-498.

Snyders DJ, Tamkun MM, and Bennett PB (1993) A rapidly activating and slowly inactivating potassium channel cloned from human heart. Functional analysis after stable mammalian cell culture expression. *J Gen.Physiol* **101**:513-543.

Tseng GN, Jiang M, and Yao JA (1996) Reverse use dependence of Kv4.2 blockade by 4-aminopyridine. *J Pharmacol.Exp.Ther.* **279**:865-876.

Uebele VN, England SK, Chaudhary A, Tamkun MM, and Snyders DJ (1996) Functional differences in Kv1.5 currents expressed in mammalian cell lines are due to the presence of endogenous Kv beta 2.1 subunits. *J Biol.Chem.* **271**:2406-2412.

Uebele VN, England SK, Gallagher DJ, Snyders DJ, Bennett PB, and Tamkun MM (1998) Distinct domains of the voltage-gated K^+ channel Kv beta 1.3 beta-subunit affect voltage-dependent gating. *Am J Physiol* **274**:C1485-C1495.

Wang Z, Feng J, Shi H, Pond A, Nerbonne JM, and Nattel S (1999) Potential molecular basis of different physiological properties of the transient outward K^+ current in rabbit and human atrial myocytes. *Circ Res* **84**:551-561.

Wickenden AD, Jegla TJ, Kaprielian R, and Backx PH (1999) Regional contributions of Kv1.4, Kv4.2, and Kv4.3 to transient outward K^+ current in rat ventricle. *Am J Physiol* **276**:H1599-H1607.

Wirth KJ, Paehler T, Rosenstein B, Knobloch K, Maier T, Frenzel J, Brendel J, Busch AE, and Bleich M (2003) Atrial effects of the novel K(+)-channel-blocker AVE0118 in anesthetized pigs. *Cardiovasc.Res.* **60**:298-306.

Wolf PA, Mitchell JB, Baker CS, Kannel WB, and D'Agostino RB (1998) Impact of atrial fibrillation on mortality, stroke, and medical costs. *Arch.Intern.Med.* **158**:229-234.

Xu H, Guo W, and Nerbonne JM (1999) Four kinetically distinct depolarization-activated K^+ currents in adult mouse ventricular myocytes. *J Gen.Physiol* **113**:661-678.

Zhou J, Jeron A, London B, Han X, and Koren G (1998) Characterization of a slowly inactivating outward current in adult mouse ventricular myocytes. *Circ Res* **83**:806-814.

Footnotes

Joachim R. Ehrlich was supported by Nachlass Martha Schmelz, Dr. Paul und Cilli Weill-Stiftung and Deutsche Forschungsgemeinschaft (EH201/2-1). The contributions of Pierre Coutu and Stanley Nattel were supported by grants from Natural Sciences and Engineering Research Council, Canadian Institutes of Health Research and the Quebec Heart and Stroke Foundation.

JPET Fast Forward. Published on August 17, 2006 as DOI: 10.1124/jpet.106.110080
This article has not been copyedited and formatted. The final version may differ from this version.

Legends for figures

Figure 1

Biophysical current characterization. **A**, $I_{K,PO}$ recorded with 1,000-ms depolarizations from a holding potential of -80 mV to potentials between 0 and +60 mV (protocol in inset, 0.1 Hz). **B**, mean±SEM $I_{K,PO}$-voltage relationship (n=20). **C**, voltage-dependence of steady-state inactivation with 1,000-ms pre-pulses to various potentials and 750-ms test-pulses to +60 mV. **D**, mean±SEM data for voltage-dependence of $I_{K,PO}$ activation and inactivation (n=10 each). **E**, mean±SEM time to peak $I_{K,PO}$ and inactivation time-constants (n=10 each). **F**, example of $I_{K,PO}$ recovery from inactivation. **G**, mean±SEM current during the 2nd pulse (I_{P2}) normalized to current during the first pulse (I_{P1}), as a function of P1-P2 interval (protocol in inset) with bi-exponential fit to mean±SEM data (n=9). **H**, $I_{K,PO}$ during the 10th pulse (I_{P10}) to +60 mV normalized to that during 1st pulse (I_{P1}) plotted over different frequencies with and without extracellular sodium. Act. - activation; inact. - inactivation, τ_f - fast time-constant, τ_s - slow time-constant, TP - test potential.

Figure 2

Determination of Cl^- and K^+-dependence. **A**, **B**, $I_{K,PO}$ recorded from the same cardiomyocyte before (**A**) and after (**B**) substitution of external chloride with equimolar cyclamate (protocol in inset). **C**, mean±SEM data (n=5). **D**, $I_{K,PO}$-recording obtained at +60 mV with regular K^+ containing internal solution. **E**,

JPET Fast Forward. Published on August 17, 2006 as DOI: 10.1124/jpet.106.110080
This article has not been copyedited and formatted. The final version may differ from this version.

$I_{K,PO}$-recording with substitution of internal K^+ with equimolar Cs^+ from a different cell isolated from the same pig as in **D** on the same day. **F**, mean±SEM $I_{K,PO}$ density at +60 mV for (n=10 for KCl, n=9 for CsCl, P<0.001). TP – test potential

Figure 3

Pharmacological properties of $I_{K,PO}$. A, left, $I_{K,PO}$ recorded with depolarizations to +60 mV (protocol in inset) under control conditions and after the application of ascending extracellular 4-AP concentrations (only recordings at 100 µM to 10 mM shown). Note the acceleration of current inactivation with low concentrations of 4-AP suggestive of open channel block. **Right**, mean±SEM fractional block for peak to steady-state current (open symbols) and integrated area under the curve (AUC, closed symbols). Panel **B, left**, example of $I_{K,PO}$ inhibition by flecainide (traces shown are from 10 µM to 1 mM), **right**, mean±SEM fractional block. **C**, representative currents recorded before and after the application of 0.01% H_2O_2 (protocol in inset). **Right panel**, mean±SEM $I_{K,PO}$-voltage relations (n=3). **D**, **left**, $I_{K,PO}$-recordings before and after the application of 10 mM TEA and mean±SEM data (n=9, **right**). Fits shown are to mean±SEM data. All protocols were delivered at 0.1 Hz, dashed lines represent zero-current level, AUC – area under the curve, TP - test potential, CTL – control, flec. - flecainide.

Figure 4

Inhibition by Kv1.5 blockers. Effects of ascending perhexiline concentrations on $I_{K,PO}$ are shown in **A** (protocol in inset) with mean±SEM fractional block (n=9,

B). **C**, representative currents from a cell exposed to various concentrations of AVE0118, **D**, mean±SEM fractional block (n=8). Fits shown are to mean±SEM data. CTL – control

Figure 5

Consequence of $I_{K,PO}$ blockade on action potentials. Effect of externally applied 0.1 mM 4-AP on action potentials (AP) recorded from single cells in current-clamp mode. **A**, representative APs before and after 4-AP application. Washout in dashed lines. **B**, mean±SEM AP duration measured at -50 and -70 mV (n=5). * P<0.05, CTL – control

Figure 6

mRNA expression of Kv channel subunits. Relative expression of Kv subunits normalized to the expression of 18S. **A**, mean±SEM data from 6 animals. **B**, representative amplification plots of real-time PCR reactions (double reaction sets) for the subunits tested. The indicator line was individually adjusted to obtain the respective Ct value for each experiment. * P<0.001.

JPET Fast Forward. Published on August 17, 2006 as DOI: 10.1124/jpet.106.110080
This article has not been copyedited and formatted. The final version may differ from this version.

Table - Primers for real-time RT PCR

Clone	**GenBank accession #**		
KCNA5	NM001006593	forw.	5'-*CCTTGTCATCCTCATCTCCATCA*-3'
		rev.	5'-*GCAGCAGCTCGCGTTCAT*-3'
		probe	5'-*CCTTCTGCTTGGAGACCCTGCCTGA*-3'
KCNA4	DQ285633	forw.	5'-*AATGAGGAACAGACACAGCTGACA*-3'
		rev.	5'-*AGAAGTAGAGCTCCGAAATTTCTTCA*-3'
		probe	5'-*TGCAGTCAGTTGCCCATACCTCCCTTC*-3'
KCND2	DQ285631	forw.	5'-*CACTTGCTGTTCAAGACGACACA*-3'
		rev.	5'-*CATCTAATCTGAATCGTGCTGAGTTC*-3'
		probe	5'-*CCAATGTATCAGGAAGCCACCGAGGC*-3'
KCND3	DQ285632	forw.	5'-*GCATGGAGAGTTCAATGCAGAA*-3'
		rev.	5'-*AGCAGCAGGTGGTGGTGAG*-3'
		probe	5'-*CACACGGAGTCCCTCGCTGTCCA*-3'
KCNIP2	DQ285634	forw.	5'-*CGACAGCGTGGAGGATGAGT*-3'
		rev.	5'-*TTGCAATTCCTTGCGTGTGA*-3'
		probe	5'-*TTGGTTTGCTCCTGCAGCTGCTCC*-3'

forw. – forward primer, rev. – reverse primer.

JPET Fast Forward. Published on August 17, 2006 as DOI: 10.1124/jpet.106.110080
This article has not been copyedited and formatted. The final version may differ from this version.

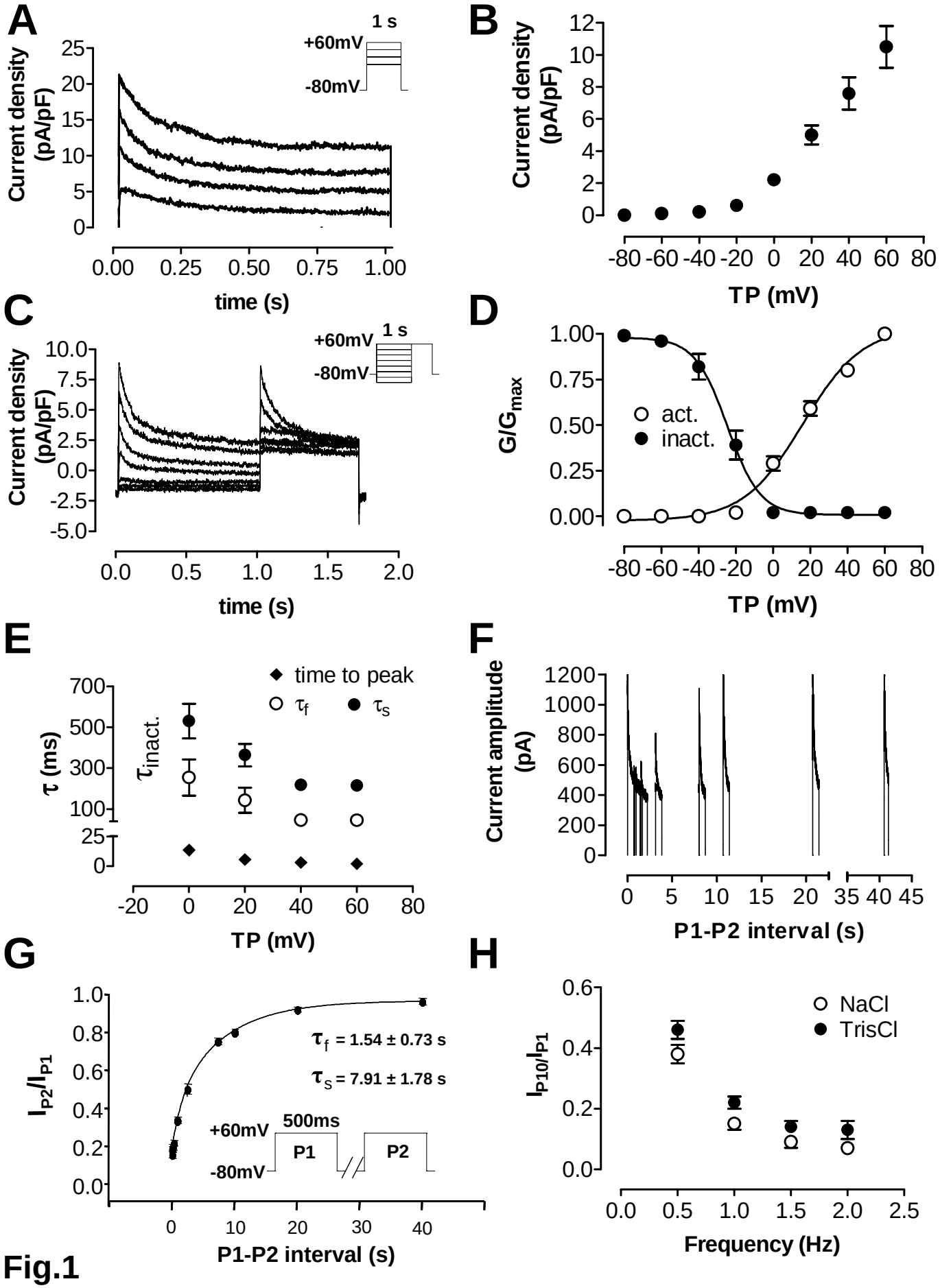

Fig.1

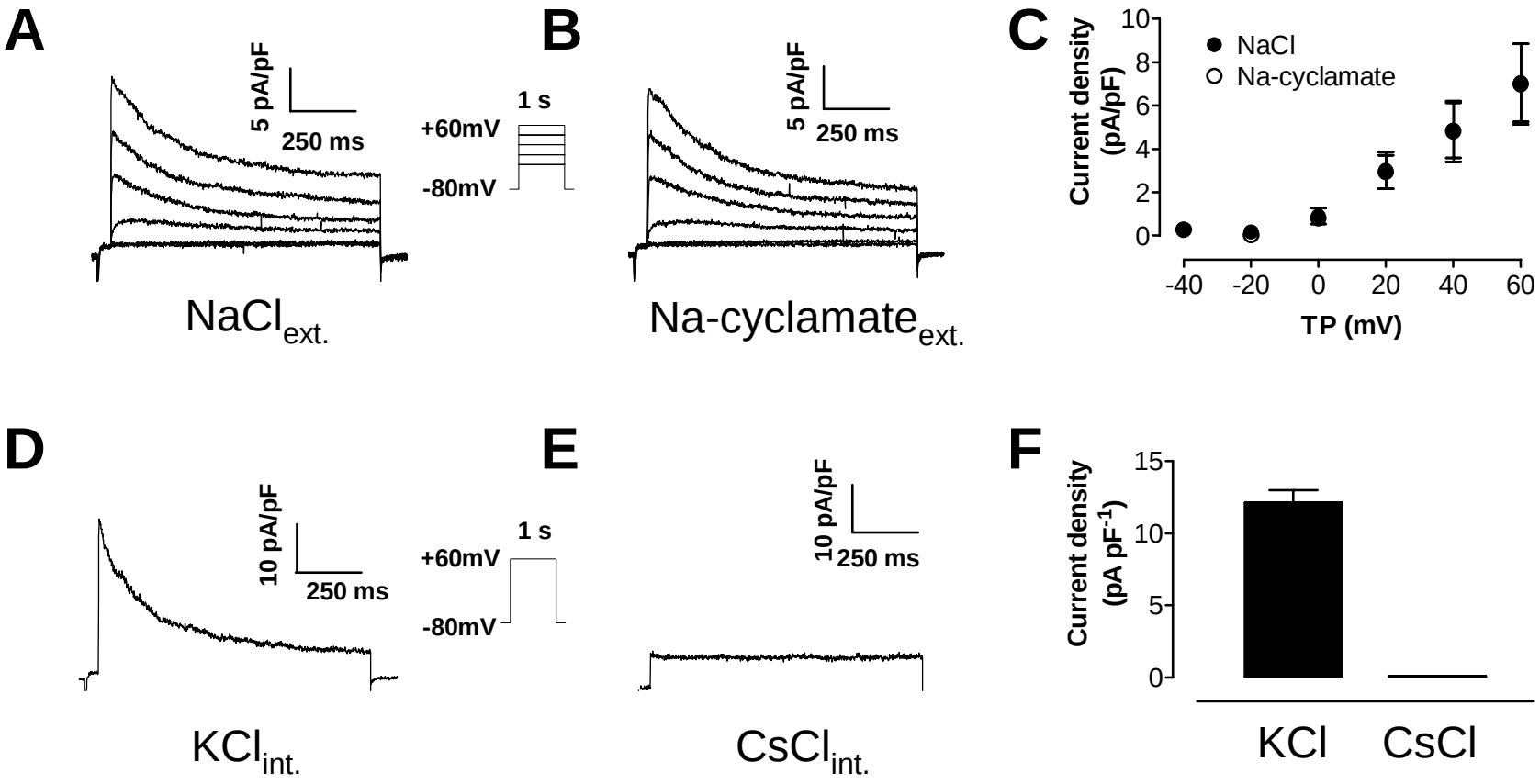

Fig.2

JPET Fast Forward. Published on August 17, 2006 as DOI: 10.1124/jpet.106.110080
This article has not been copyedited and formatted. The final version may differ from this version.

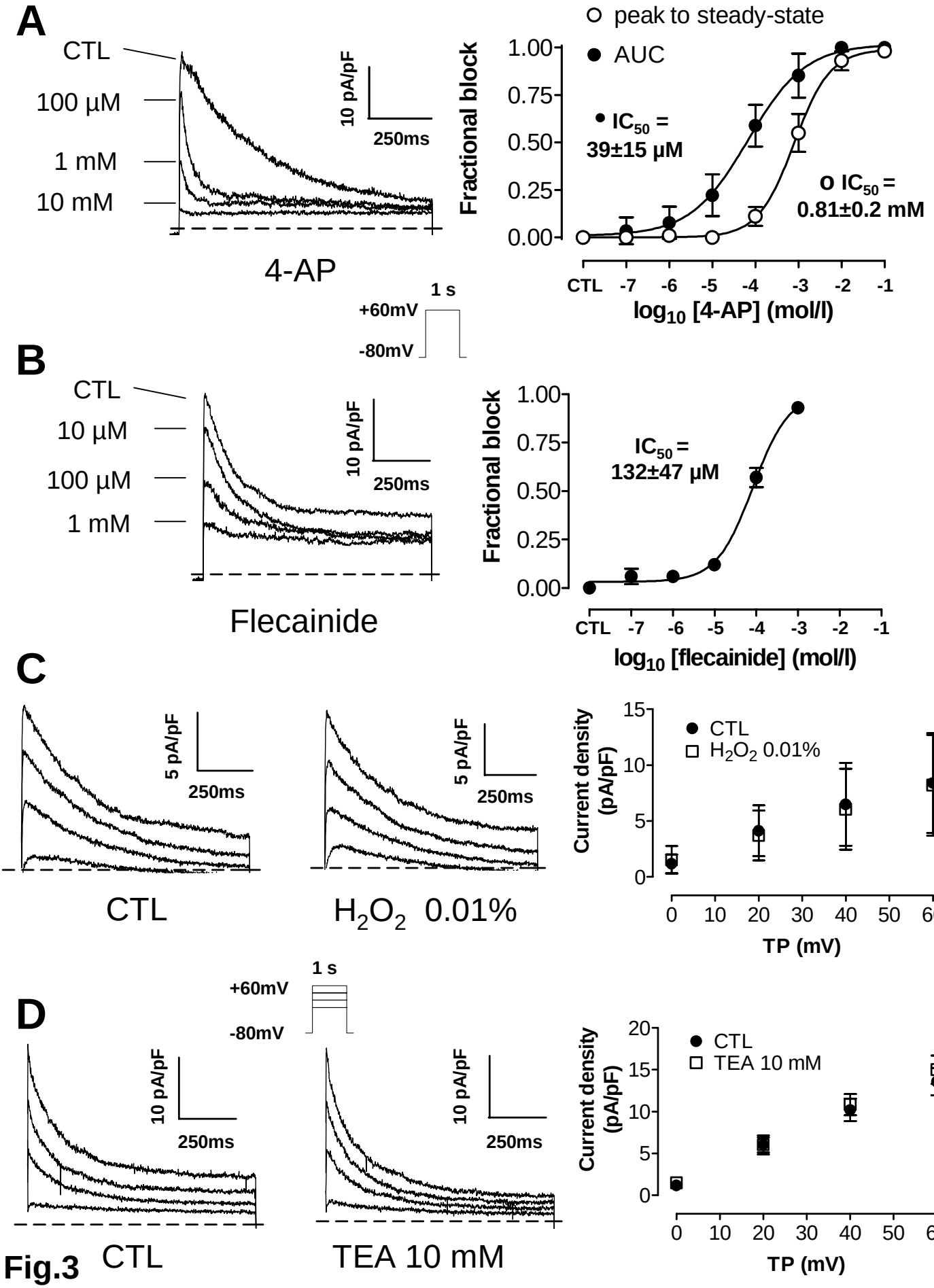

Fig.3

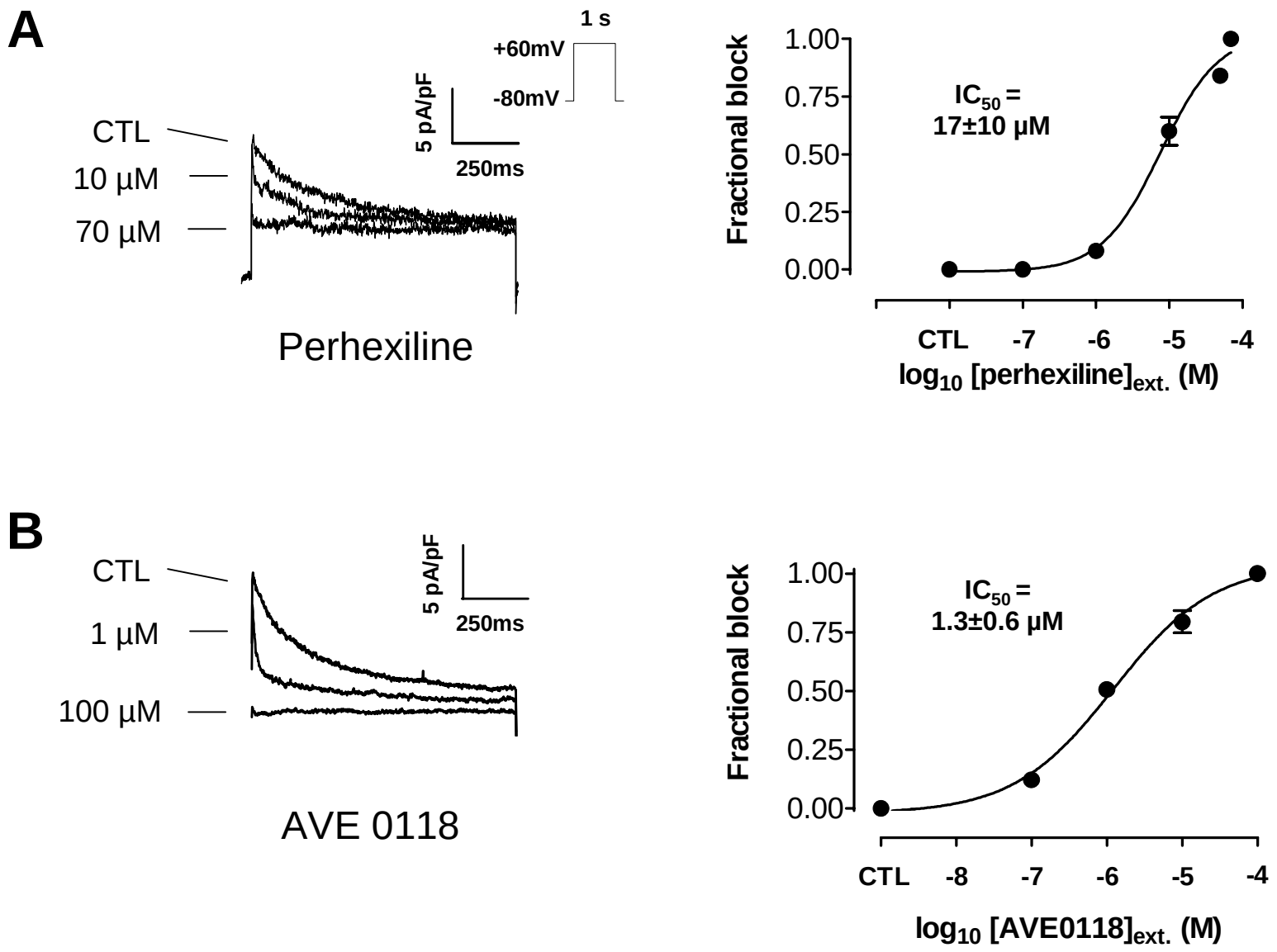

Fig.4

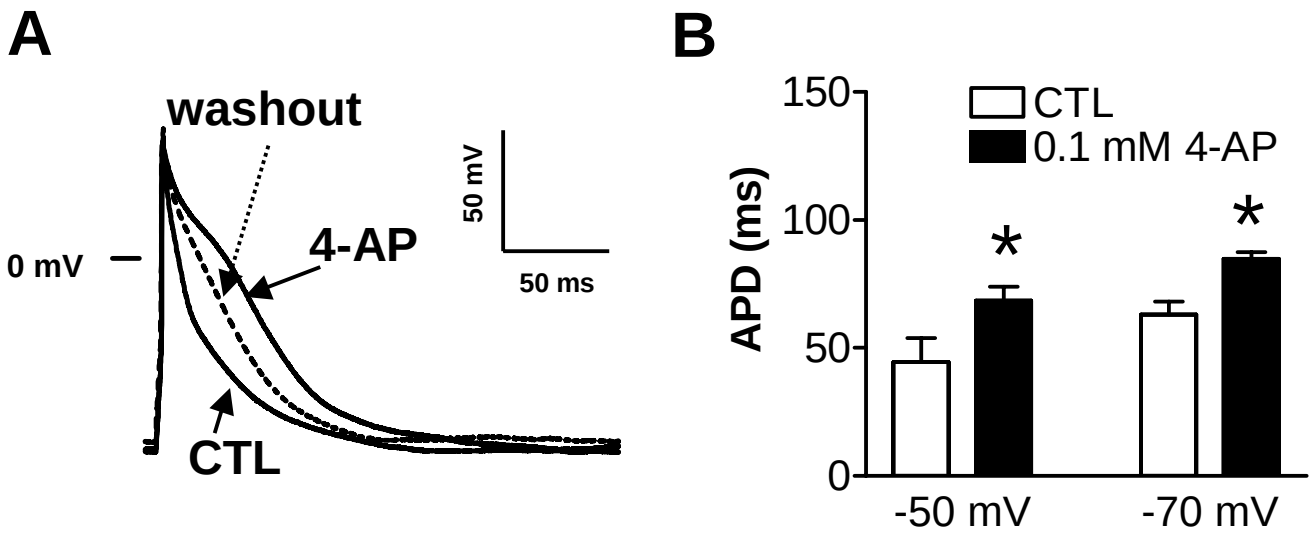

Fig.5

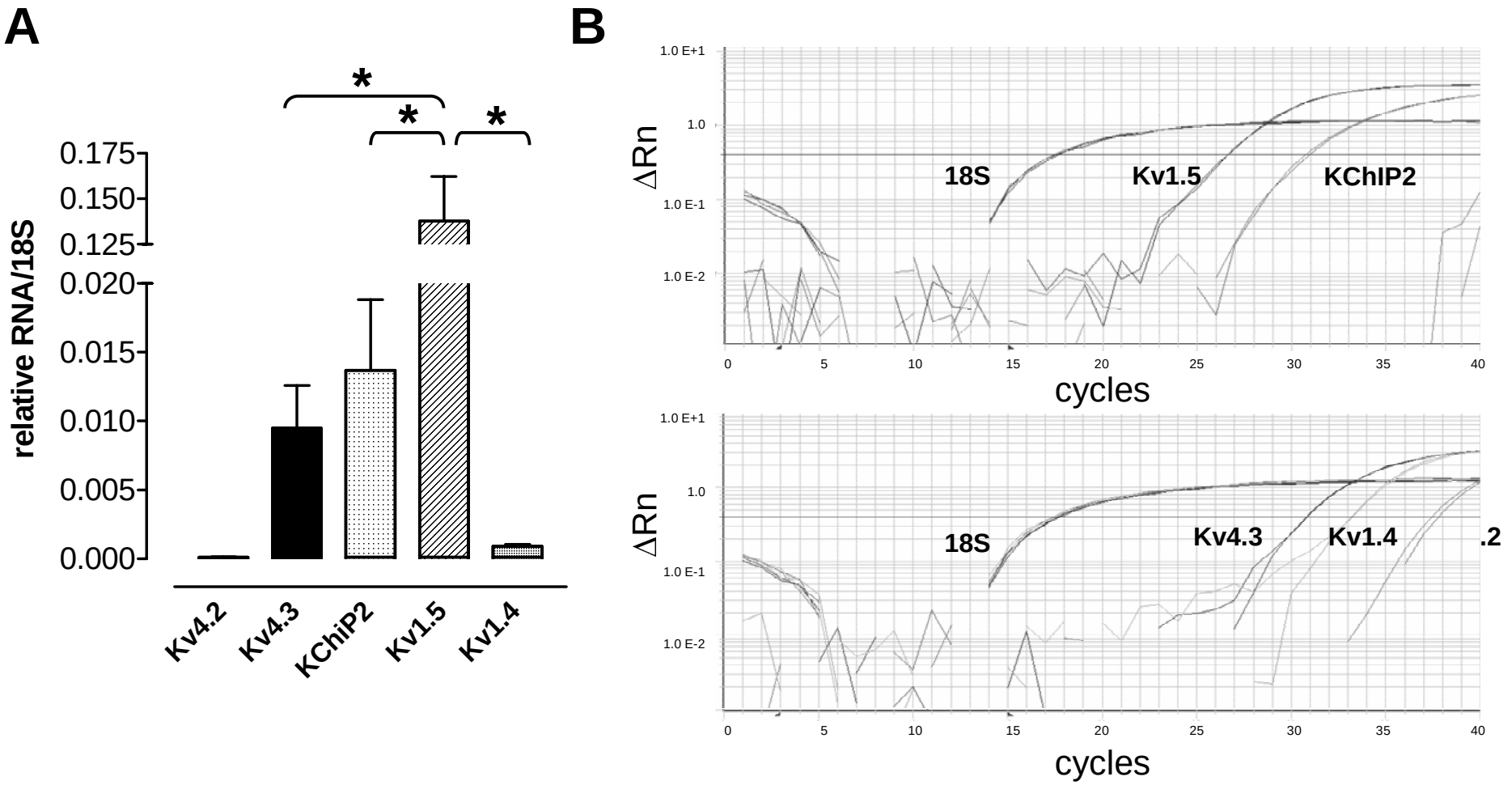

Fig.6